Draft version March 20, 2007
Preprint typeset using LaTeX style emulateapj v. 11/12/01

AN UNUSUAL CIRCUMSTELLAR DEBRIS STRUCTURE ASSOCIATED WITH THE NEARBY, SUN-LIKE STAR HD 61005

Dean C. Hines[1], Glenn Schneider[2], Stanimir A. Metchev[3], Lynne A. Hillenbrand[4], Eric E. Mamajek[5], Michael R. Meyer[2], Jeroen Bouwman[6], John M. Carpenter[4], Thomas Henning[6], Jinyoung Serena Kim[2], Joan Najita[7], Murray D. Silverstone[8], Jens Rodmann[6], Sebastian Wolf[6]

Draft version March 20, 2007

ABSTRACT

We present the discovery of an unusual circumstellar structure associated with the 50-150 Myr old, nearby (34.6±1.1 pc), sun-like G-dwarf star HD 61005. *Spitzer* IRAC, IRS & MIPS observations, conducted as part of the FEPS *Spitzer* legacy science survey of sun-like stars, detail the nature of thermal emission from the object that is in excess of the expected stellar photosphere. Follow-up 0.″1 spatial resolution *HST*/NICMOS 1.1 μm coronagraphic images reveal a very bright structure (flux density $\sim 18 \pm 3.3$ mJy, $0.65\% \pm 0.12\%$ that of the $J_{mag} = 6.91$ star) that scatters starlight to distances as far as 7″ ($\sim$ 240 AU) from the occulted star. The structure exhibits a strong asymmetry about its morphological major axis, but is mirror-symmetric about its minor axis (invision a wing-spread moth with the star as the head). The scattered light is traced inward to within 10 AU of the star (limited by the coronagraphic obscuration) with no evidence of a turnover in radial surface brightness profiles. The fraction of 1.1 μm starlight scattered by the structure at $r > 0.''3$ is larger than any debris disk previously observed, and exceeds that of β Pictoris by more than a factor of 2. Despite having a fairly typical infrared SED for a debris system, this extended structure is unlike any other previously imaged.

Subject headings: circumstellar matter — infrared: stars — planetary systems: protoplanetary disks — stars: individual (HD 61005)

1. INTRODUCTION

Our knowledge of the formation and evolution of planetary systems has evolved rapidly within the last two decades. The landmark discovery made with *IRAS* of excess IR emission associated with the A-star Vega (Aumann et al. 1984) proved conclusively that circumstellar material analogous to the debris found in our solar system can exist around another main sequence star. Subsequent *IRAS* and *ISO* detections of stars with IR excesses (e.g., Mannings & Barlow 199*; Spangler et al. 2001)[9] showed that debris, presumably arrising from colliding planetasimals, is fairly common (e.g., Lagrange et al. 2000; Meyer et al. 2007).

The *Spitzer* Space Telescope Legacy Science program entitled the Formation and Evolution of Planetary Systems (FEPS) was designed to extend the earlier *IRAS* and *ISO* results to sun-like stars of spectral types F8V through K3V and ages from 3 Myr to 3 Gyr (Meyer et al. 2004; 2006). The FEPS survey has now successfully identified many new candidate debris systems with infrared emission in excess of that expected from the stellar photospher (Meyer et al. 2004; Kim et al. 2005; Hines et al. 2006; Hillenbrand et al. 2007; Carpenter et al. 2007).

Models of the spectral energy distributions (SEDs) of these newly identified debris systems place constraints on the temprature and size distribution of the material, but cannot uniquely determine the spatial distribution; the objects are unresolved by *Spitzer*. Single-dish sub-mm observations are limited to spatial resolutions of 10-20″, and sub-mm interferometry is so far limited to a few arcsec, comparable with *Spitzer*. Currently, only high spatial resolution (sub-arcsecond) images of scattered light can address questions such as: 1) the exact radial extent of the material; 2) the grain surface density distribution; and 3) whether the disk exhibits azimuthal asymmetries indicative of particle shepherding by unseen planets.

Therefore, we have begun extensive followup observations of FEPS-identified debris systems using the *HST*/NICMOS (near-IR) coronagraph to look for, spatially map, and obtain surface brightness measurements of starlight-scattering, circumstellar material. Here we report images of 1.1μm light scattered by material in the close circumstellar environment of the 50-150 Myr old, late G dwarf star, HD 61005 [HIP 36948, SAO 198166; d = 34.6 ± 1.1 pc (Perryman 1997)]. The remarkable structure revealed by these observations is unlike any other debris systems observed previously.

2. OBSERVATIONS

[1] Space Science Institute, 4750 Walnut Street, Suite 205 Boulder, CO 80301.
[2] Steward Observatory, The University of Arizona, 933 N. Cherry Ave., Tucson, AZ 85721.
[3] University of California, Los Angeles, CA.
[4] Astronomy, California Institute of Technology, Pasadena, CA 91125.
[5] Harvard-Smithsonian Center for Astrophysics, 60 Garden Street, Cambridge, MA 02138.
[6] Max-Planck-Institut fur Astronomie, Konigstuhl 17, D-69117 Heidelberg, Germany.
[7] National Optical Astronomy Observatories, AURA
[8] Eureka Scientific, 10813 Graeloch Road, Laurel, MD 20723-1124.
[9] The sensitivity of both missions limited discovery primarily to fairly luminous, A & F, dwarf stars and younger pre-main-sequence stars.

HD 61005 was observed in the FEPS survey (PID 148) with all three science instruments on the *Spizter* Space Telescope (Werner et al. 2004) using the procedures described in detail by Meyer et al. (2006). Reduction of the data followed the detailed procedures used for the entire FEPS survey (Carpenter et al. 2007) as generally outlined in previously FEPS contributions (Kim et al. 2005; Hines et al. 2006; Bouwman et al. 2007).

IRAC and MIPS[10] photometry for HD 61005 are presented in Table 1, along with synthetic photometry at 13, 24 and 33 μm derived from a low (spectral) resolution IRS spectrum using rectangular FWHM band-passes of 1.6, 4.7 and 5 μm, respectively. These IRS flux densities are the error–weighted means within each passband. Table 1 also includes a 60 μm detection from *IRAS* (HD 61005 was not detected in the other three *IRAS* bands).

HD 61005 was observed with the coronagraph in NICMOS camera 2 (scale: 75.8 mas pixel^{-1}) using the F110W (λ_{eff} = 1.104 μm, FWHM = 0.5914 μm) filter. Coronagrahic images were obtained at two celestial orientations differing by 131 degrees in the frame of the camera 2 detector. Such observations enabling post-processing discrimination against, and reject of, rotationally invariant optical artifacts in imperfect PSF subtracted images (notably residuals from the HST diffraction spikes, but other artifacts as well). The observing strategy, data calibration methodology and reduction techniques follow those outlined in Schneider, Hines & Silverstone 2005 (SSH05) used successfully in HST GO program 10177 (PI: Schneider). Details of the HD 61005 observing plan are captured in the publicly available Phase II definition of the GO 10527 program[11].

Instrumentally calibrated count rate images were created from the individual F110W coronagraphic multiaccum frames. For each target/visit (orientation) the individual images were median combined after verifying the repeatability of the intra-visit images within the typical range of inter-image stability. Following SSH05, well characterized instrumentally induced artifacts associated with the detector/readout electronics were removed in image calibration and processing. This was also done for all targets in the GO 10527 program including those of the PSF template observations later applied to the HD 61005 observations.

All similarly processed and instrumentally calibrated count rate images obtained in the GO 10527 program that showed no evidence of scattered light excesses themselves were tested for suitability as PSF templates. The efficacy of PSF subtractions requires target/template PSFs to be (*a*) well matched in J-H color index (usually |J-H |$\leq$ 0.3), (*b*) roughly comparable "breathing" phase space (relative *HST* secondary mirror despace excursions $\lesssim 1\mu$m; as empirically determined from residual PSF structure), and (*c*) close repeatability of the NICMOS camera 2 cold mask position (which has small thermally driven metrologic instabilities). For the first orientation HD 61005 observation (denoted "Visit16") ten suitable template PSF were found from the GO 10527 target set, and five for the Visit 15 (second orientation) observation. All images were co-registered in detector coordinates about the location of HD 61005 image in the Visit 16 image and corrected for the $\sim 0.7\%$ linear geometrical distortion in Camera 2. All images were flux scaled (initially) to an F110W magnitude of 5.0 based upon 2MASS catalog photometry transformed from J-band using the *calcphot* task in the STSDAS package. In doing so we assumed stellar spectral types as given via SIMBAD. The F110W transformed catalog magnitudes were cross-checked as described in SSH05 using "TinyTim" model PSFs matched in intensity to wings of short, but core-saturated, contemporaneously obtained non-coronagraphic images of the stars. The individual images comprising the two sets of PSF templates (one set of ten and one set of five) were subtracted from their paired HD 61005 observations, resulting in fifteen PSF-subtracted images of HD 61005.

Artifact (diffraction spike and other low-spatial frequency mis-matched PSF subtraction residual) rejection masks were individually made for the full set PSF subtracted images. The two sets of HD 61005 PSF-subtracted masked images from each orientation were, separately, median combined (rejecting pixels for each image based upon the masks before median combination). This resulted in two artifact-rejected median-combined PSF-subtracted images (one for each HD 61005 visit). These two images were then both rotated to a "north up" orientation, and averaged, but rejecting pixels unsampled (e.g. along diffraction spikes or other individually commonly masked masked artifacts) in either image.

As a check on the procedure, the images were combined in two ways: first by a simple (masked) mean for the two visits; and second by a weighted mean of the two visits, with 2:1 weights for visits 16 & 15 predicated upon the number of input images after pixel masking. The resulting images (as expected) differ slightly, but these differences speak to the dispersion the detailed structure of the input images. The "final" image which we speak to in the remainder of the paper is based upon the weighted mean combination.

To verify that the fidelity of the circumstellar scattered-light structure seen in the HD 61005 image, we followed the same process multiple times but choosing (each time) a different image from the PSF template set as a (null) test target in place of HD 61005. All of the resulting "PSF-minus-PSF" images showed no features bearing any resemblance to circumstellar scattered-light in the HD 61005 processed images. The dispersion in the (much lower level) remaining instrumentally diffracted and scattered light in the "PSF-PSF" images was used to assess the systematic uncertainties in the flux density measures in the HD 61005 processed images.

3. THERMAL EMISSION AND SCATTERED LIGHT

Figure 1 shows the spectral energy distribution (SED) of HD 61005. The *Spitzer* observations show a strong infrared excess above the expected stellar photopshere. For completeness we show the *IRAS* 12, 25 & 100 μm upper limits, a *IRAS* 60 μm detection, and a 1.2 mm upper limit (Carpenter et al. 2005). The stellar SED is well fit by a Kurucz model ($T_{\rm eff}$ = 5537 K, log(g) = 4.56) from the optical through $\approx 8\mu$m, but shows a strong excess for

[10] The FEPS survey did not obtain MIPS 160 μm observations for this object.

[11] http://www.stsci.edu/observing/phase2-public/10527.pdf

$\lambda > 18\mu$m. The IRS spectrum (inset in Fig. 1) does not show obvious spectral features, implying that the thermal emission does not originate from hot, small grains that would produce strong silicate emission features. Figure 1 also shows a T = 60K blackbody SED, scaled to the 24, 60 and 70 μm photometry, that yields $L_{IR}/L_* \approx 2 \times 10^{-3}$. This blackbody temperature provides a minimum distance of the material of $\gtrsim 16$ AU, using $L_*/L_\odot = 0.55$ (from integrating the best fit Kurucz model) and $M/M_\odot = 0.84$ (Nordstrm et al. 2004). Additional modeling as part of an ensemble study of FEPS identified, cool debris disks, suggests that the SED is fit by an extended ($7 \lesssim R_{dust} \lesssim 70$ AU disk, with a $\sim$ 10K dispersion in temperature around 60K (Hillenbrand et al. 2007).

Figure 2 shows the 1.1 μm scattered light image as a $\log_{10}$ color-coded contour map, with the corresponding image inset. The grey circle at image center represents the 0.″3 radius coronagraphic obscuration (corresponding to r = 10.3 AU at the distance of HD 61005). The pattern of scattered light (resembling a Moth) is asymmetric about its morphological major axis and mirror-symmetric about its minor axis. The scattered starlight extends to $\sim 3''$ (105 AU) along the minor axis to the southeast (celestial PA = 160 deg) and 5-6″ (175–210 AU) both sides of the star along the "major axis." The maximum extent of the scattered light pattern is $\sim 7''$ (the "wingtips of the Moth" below the major, and toward the minor, axis). Very little scattered starlight is detected in the northwest sector flanking the minor axis. At $r = 0.75''$, the on-axis ratio of the south to north scattered light is $\sim$ 12, and at 2 ″there is no scattered light detected above the residual background noise. The total 1.1μm flux density within an annulus from $0.''3 \leq r \leq 5''$ is F(F110W) = 18 mJy $\pm$ 3.3 mJy. This yields a 1.1μm scattering fraction $f_{disk}/f_* = 0.65\% \pm 0.12\%$.

Figure 3 presents radial surface brightness profiles for three crosscuts; one along the southern semi-minor axis, and two along the peak surface brightness ridges extending "below" the major axis on either side of the star. While we measure positive flux densities very close to the occulting edge of the coronagraphic hole, we conservatively show only the profiles for $r \geq 0.''7$ where we are confident that systematics do not dominate the result. The surface brightness profiles from $0.''7 \leq r \leq 5.''0$ along both sides of the star in the direction of the ridge of maximum brightness at $r = 5''$ are well represented by unbroken $r^{-2.5}$ and $r^{-2.7}$ power law fits for the east and west extensions, respectively. Beyond 0.″7, the surface brightness profile along the southern semi-minor axis is well fit by broken $r^{-2.0}$ and $r^{-5.0}$ power laws, for $0.''7 \leq r \leq 1.''4$, and $1.''4 \leq r \leq 2.''6$, respectively; shallower interior, and steeper exterior, to the break at $r = 1.''4$ than the profiles along the ridges of maximum brightness in the "wings of the Moth".

4. THE EVOLUTIONARY STATUS OF HD 61005

HD 61005 is reported as G0 spectral type in the Henry Draper Catalog (Cannon et al. 1993), as G3/5V in Houk et al. (1982), and as G4V in SIMBAD. Nordstrom et al. (2004) infer T_{eff} = 5346K from the Stromgren indecies, suggesting a $\sim$ G9.5 spectral type. Based on published photometric colors, we find that the spectrum is well fit by a Kurucz model with T_{eff} = 5537 K and $\log(g) = 4.56$, consistent with a G8V spectral type (Fig. 1).

Observations of CaII ($\log R'_{HK}$ = -4.275: Soderblom et al. in prep; Henry et al. 1996), Hα emission (EW(Hα) = 136 ± 6 m$\mathring{A}$: Waite et al. 2005) and soft X-ray emission ($\log (L_X L_{bol} = 29.2$: Wichmann, Schmitt & Hubrig 2003) show that HD 61005 is chromospherically active, but not actively accreting. The star does not show optical variability over a two year timescale ($\Delta V \leq 0.01$mag: Menzies, Marang, & Westerhuys 1990).

Its UVW vector (-22.9, -14.0, -4.1)($\pm$ 0.4, 0.4, 0.3) is well-constrained, and is not near where the majority of $<$ 100 Myr-old stars within 100 pc are found (i.e. Gould Belt and Pleiades "clumps"). There are no B stars with motions similar to HD 61005 within 100 pc, except for stars of type B5 and later. This at least suggests that the motion of HD 61005 would be somewhat unusual compared to that of stars with ages of $\lesssim$ 80 Myr within 100 pc of the Sun. Interestingly, though, its UVW vector is almost exactly coincident (within 2 km/s) with the $\sim$ 50-Myr-old $\sim$ 150-pc-distant IC 2391 open cluster (-22.9, -13.6, -6.0)($\pm$ 0.8, 0.3, 0.2) (Robichon et al. 1999). To appreciate how close this is, out of 13239 stars in the Nordstrom et al. (2004) catalog with UVW vectors, only 3 (0.02%) have UVW space motions closer to IC 2391 than HD 61005.

The CaII H&K emission suggests $t_{star} \sim 125$ Myr using a range of calibrations (Soderblom et al. 1991; Donahue et al. 1993; Lachaume et al. 1999; Mamajek, private comm.), and the lithium absorption (EW(Li) = 164 mÅ: Wichmann, Schmitt & Hubrig 2003) implies $t_{star} \sim 50$ Myr (REF). Given these indicators and the space motion, we estimate the age to be $50 \leq t_{star} \leq 150$.

5. THE CIRCUMSTELLAR MATERIAL ASSOCIATED WITH HD 61005

Although the near-IR scattered light image is remarkably similar to that observed for the classical T-Tauri star GM Aur (Schneider et al. 2003), the SED, including the lack of infrared excess at $\lambda \lesssim 8\mu$m, argues against T-Tauri-like disk. Furthermore, the optically thick disks around pre-main-sequence stars TW Hydrae (Weinberger et al. 199*) and Hen 3-600 (RayJay et al. ****) in the $t_{star} \sim 10$ Myr old TW Hydra Association (TWA) both show thermal emission over a large range of temperatures, with large Lir/Lstar (****).

The estimated age of HD 61005 also argues against this interpretation, since the oldest T-Tauri objects are $\sim 20 - 30$ Myrs (REF). If HD 61005 does posses an optically thick disk, it would be the oldest example known by at least a factor of two. Instead, we suggest that the material associated with HD 61005 is debris that is being replenished by the erosion/collision of planetesimals orbiting the star. We speculate that unusual morphology of the scattered light arises from material that has been created recently by a catastrophic event.

The timescale for grain migration due to PR-drag is about one thousand times longer than the collision time; the evolution of material around HD 61005 is dominated by collisions, and the loss of material from the system is dominated by grain blow out. While the majority of the material responsible for the thermal emission could be undergoing more gentile cascading erosion as witnessed in

the solar system and other debris systems, the strongly asymmetric scattered light image suggests that the scatterers are not dynamically relaxed. The extended scattered emission we see in HD 61005 could thus be caused by very small grains (below the blowout size of $\sim 0.5\mu$m) that were created in the breakup of a massive (icy) body (the deep impact mission showed that the comet was very loosely packed and produced a HUGE dust cloud... much bigger, dustier and brighter than expected). The blowout time is ~ 100 yrs, similar to the orbital time scales at the distance of 50 pc. The majority of the thermal emission could from larger grains in a more traditional debris disk, closer to the star.

I WORRY THAT WE CONTINUE TO INVOKE "CAUGHT IN THE ACT" ARGUMENTS... BUT PERHAPS THIS IS OK, GIVEN THE STOCHASTIC NATURE OF THE A-STAR RESULST... A comparison between mass estimates for the scatterers and thermally emitting dust would be interesting.

6. CONCLUSION

We have discovered a very unusual circumstellar structure associated with the $50 - 150$ Myr old, sun-like star HD 61005. In particular:

- The structure seen in scattered 1.1μm light is highly asymmetric, resembling the morphology of an optically thick, inclined T-Tauri disk rather than the optically thin, debris disks and rings seen in other stars of similar age with thermal infraed excesses.
- Despite its morphology, the thermal SED and the age of the system suggest that the material is associated with debris rather than remnants of the primordial disk.
- The fraction of 1.1μm starlight scattered by the structure at $r > 0\farcs3$ is larger than any debris disk previously observed, and exceeds that of β Pictoris by more than a factor of 2.

The observations lead us to speculate that we are witnessing the very recent destruction of a comet or KB-like object that produced copious small grains, which are being blown out of the system. New data such as planned, *HST* multi-wavelength coronagraphic polarimetry, together with more *Spitzer* (and future Herschel) data will further elucidate the nature of this object.

This investigation was based [in part] on observations made with the NASA/ESA Hubble Space Telescope, obtained at the Space Telescope Science Institute (STScI), which is operated by the Association of Universities for Research in Astronomy, Inc., under NASA contract NAS 5-26555. These observations are associated with program GO10527, support for which was provided by NASA through a grant from STScI. This work is also based [in part] on observations made with the Spitzer Space Telescope, which is operated by the Jet Propulsion Laboratory, California Institute of Technology under NASA contract 1407. FEPS is pleased to acknowledge support from NASA contracts 1224768 and 1224566 administered through JPL. This publication makes use of data products from the Two Micron All Sky Survey, which is a joint project of the University of Massachusetts and the Infrared Processing and Analysis Center/California Institute of Technology, funded by the National Aeronautics and Space Administration and the National Science Foundation. We have also made use of the SIMBAD database.

REFERENCES

Aumann, H. H., et al. 1984, ApJ, 278, L23
Butler, R. P., et al. 2006, ApJ, 646, 505
Cannon, A. J., & Pickering, E. C. 1993, VizieR Online Data Catalog, 3135, 0
Carpenter, J. M., Wolf, S., Schreyer, K., Launhardt, R., & Henning, T. 2005, AJ, 129, 1049
Henry, T. J., Soderblom, D. R., Donahue, R. A., & Baliunas, S. L. 1996, AJ, 111, 439
Hines, D. C., et al. 2006, ApJ, 638, 1070
Houk, N. 1988, Michigan Catalogue of Two-dimensional Spectral Types for the HD Stars (Ann Arbor : Univ. Michigan; distributed by University Microfilms International)
Kalas, P., Graham, J. R., Clampin, M. C., & Fitzgerald, M. P. 2006, ApJ, 637, L57
Kim, J. S., et al. 2005, ApJ, 632, 659
Lagrange, A.-M., Backman, D. E., & Artymowicz, P. 2000, Protostars and Planets IV, 639
Low, F. J., Smith, P. S., Werner, M., Chen, C., Krause, V., Jura, M., & Hines, D. C. 2005, ApJ, 631, 1170
Marcy, G. & Butler, P. 1998, ARAA, 36, 57
Mason, B. D., Henry, T. J., Hartkopf, W. I., Ten Brummelaar, T., & Soderblom, D. R. 1998, AJ, 116, 2975
Menzies, J. W., Marang, F., & Westerhuys, J. E. 1990, South African Astronomical Observatory Circular, 14, 33
Meyer, M. R., & Beckwith, S. V. W. 2000, LNP Vol. 548: ISO Survey of a Dusty Universe, 548, 341
Meyer, M. R., et al. 2004, ApJS, 154, 422
Meyer, M. R., et al. 2006, PASP, 118, 1690
Meyer, M. R., Backman, D. E., Weinberger, A. J., & Wyatt, M. C. 2007, Protostars and Planets V, 573
Nordström, B., et al. 2004, A&A, 418, 989
Perryman, M. A. C. & ESA 1997, The Hipparcos and Tycho catalogues. ESA SP Series Vol. 1200
Rocha-Pinto, H. J., & Maciel, W. J. 1998, MNRAS, 298, 332
Schneider, G., et al. 1999, ApJ, 513, L127
Schneider, G., & Stobie, E. 2002, in ASP Conf. Ser. 281, ADASS XI, ed. D. A. Bohlender, D. Durand, & T. H. Handley (San Francisco: ASP), 382
Schneider, G., Silverstone, M. D., & Hines, D. C. 2005, ApJ, 629, L117
Schneider, G., et al. 2006, ApJ, 650, 414
Smith, P. S., Hines, D. C., Low, F. J., Gehrz, R. D., Polomski, E. F., & Woodward, C. E. 2006, ApJ, 644, L125
Soderblom, D. R., Henry, T. J., Shetrone, M. D., Jones, B. F., & Saar, S. H. 1996, ApJ, 460, 984
Soderblom, D. R., et al. 1998, ApJ, 498, 385
Soderblom, D. R., King, J. R., Hanson, R. B., Jones, B. F., Fischer, D., Stauffer, J. R., & Pinsonneault, M. H. 1998, ApJ, 504, 192
Waite, I. A., Carter, B. D., Marsden, S. C., & Mengel, M. W. 2005, Publications of the Astronomical Society of Australia, 22, 29
Werner, M. W., et al. 2004, ApJS, 154, 1
White, R.J., Gabor, J. & Hillenbrand, L.A. 2006, ApJ, in press
Wichmann, R., Schmitt, J. H. M. M., & Hubrig, S. 2003, A&A, 399, 983

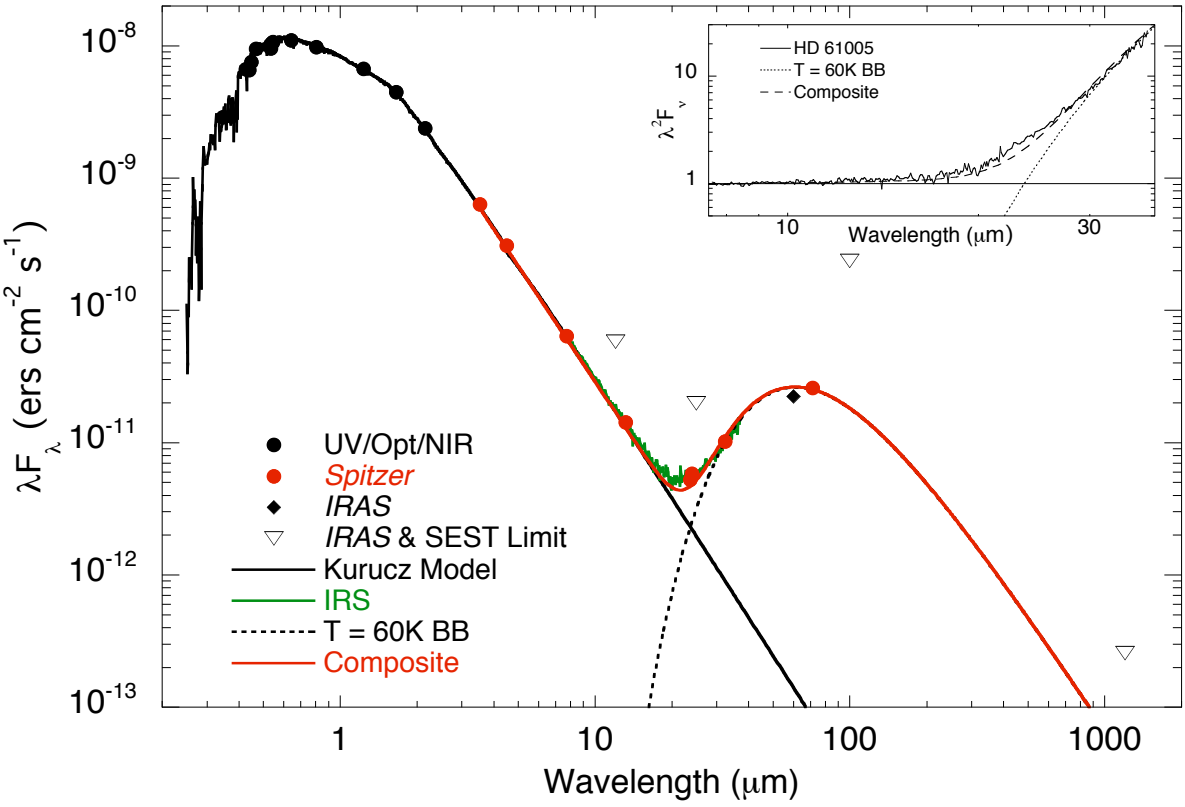

FIG. 1.— The spectral energy distribution of HD 61005. The upper panel shows the Kurucz model that best fits the optical and near-IR photometry (solid curve), the ground and space-based photometry (solid symbols) and the IRS spectrum (green curve). The 1σ error bars for each point are smaller than the symbol sizes. We also show upper limits from *IRAS* at 12, 25 and 100μm. Also shown is a T = 60K blackbody. The inset shows the observed IRS spectrum multiplied by λ^2 and normalized at 7.5μm. The spectrum clearly deviates from Rayleigh-Jeans for $\lambda \geq 18\mu$m. The apparent offset for $\lambda \gtrsim 12\mu$m may be caused by residual order mismatch in the IRS spectrum.

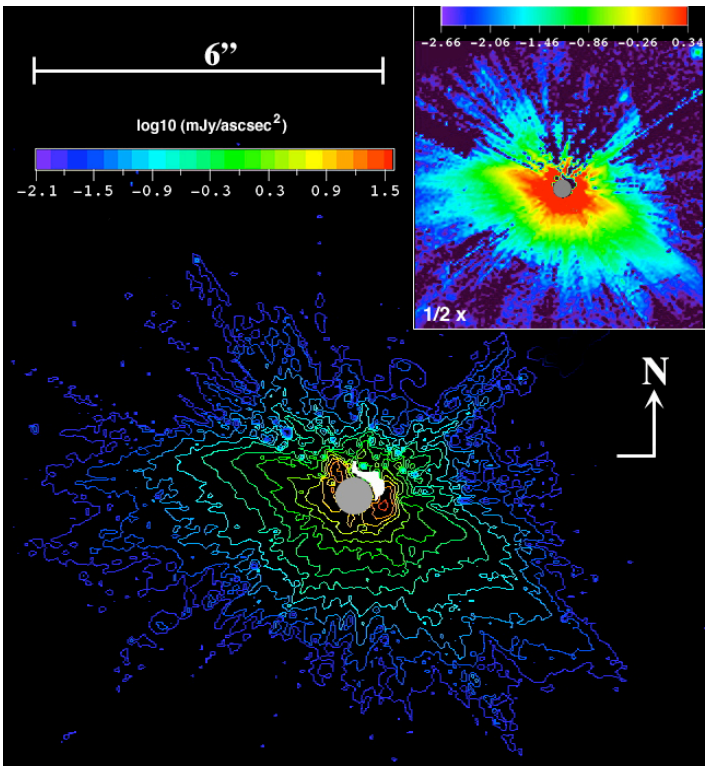

FIG. 2.— 1.1 μm $\log_{10}$ isophotal contour map of the circumstellar region about HD 61005 derived from the two-orientation combined PSF-subtracted coronagraphic image (image inset at half spatial scale). Surface brightness countor intervals every [0.3] dex from 7.9 μJy arcsec^{-2} to 31.6 mJy arcsec^{-2}. Log_{10} image inset stretch from 2.18 μJy arcsec^{-2} to 2.18 mJy arcsec^{-2}. Central grey circle represents the $r = 0\farcs3$ coronagraphic obscuration. The small region immediately adjacent to the obscuration to the NW (masked white in contour map, black in image) is invalid due to residual image artifacts at that location.

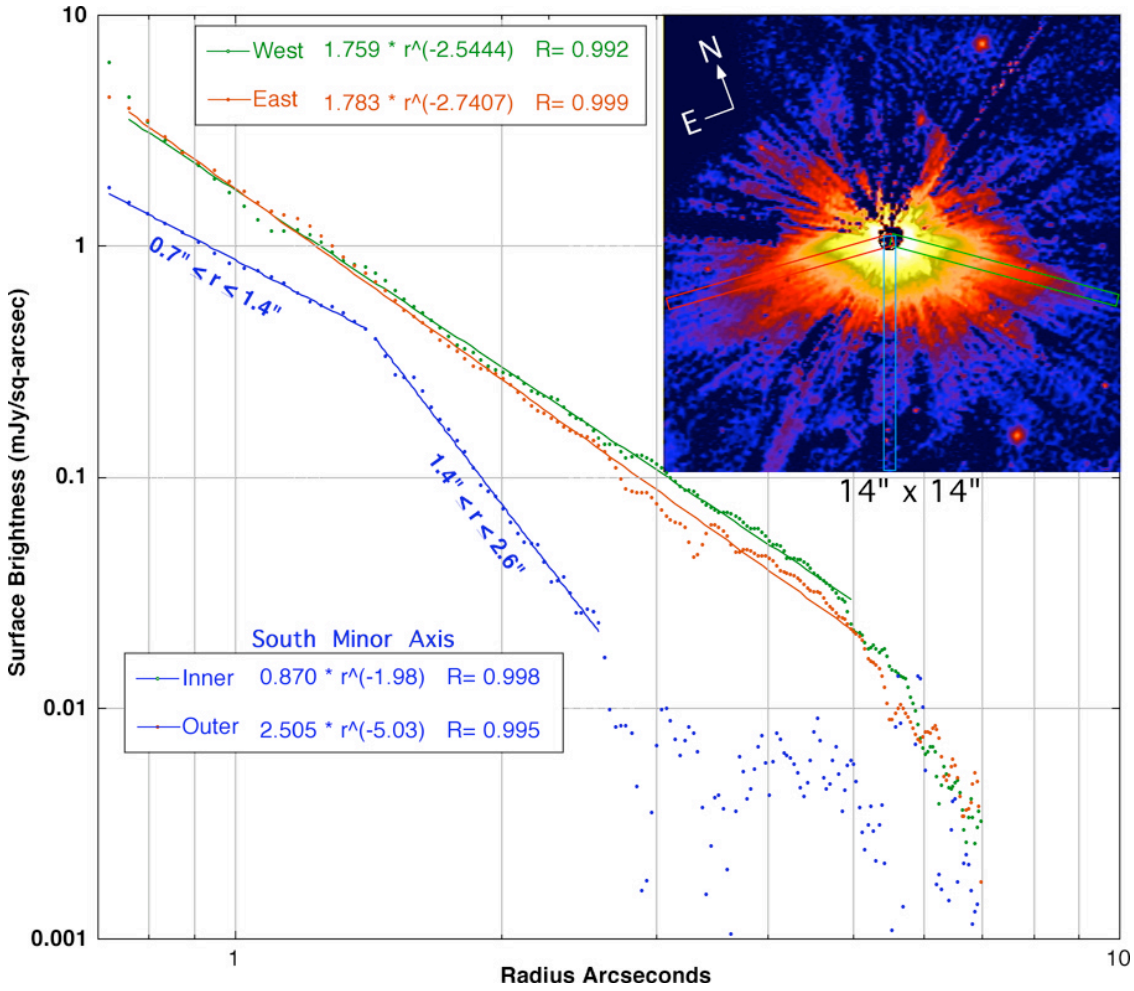

FIG. 3.— The radial decline in the scattered starlight surface brightness (measured in 0.″38 wide radial slices) falls off symmetrically with respect to the minor axis outward from the location of the star. In the directions of the maximum extent of the scattered-light pattern (red and green "cuts" overlaid on the image inset), the surface brightness declines as $r^{-2.6\pm0.1}$ from 0.″7 to 5.″0. Along the southern minor axis, the surface brightness declines as $r^{-2.0}$ from 0.″7 to 1.″4 and as $r^{-5.0}$ from 1.″4 to 2.″6. The outer part of the scattering region shown in red in the image inset is detected with $> 3\ \sigma$ per pixel significance and corresponds to the outer blue contours in Figure 2. Beyond, additional scattered light is seen declining to levels of a few μmJy arcsec^{-2} at the sensitivity limits of the observation to r $\sim 7\ ''$.

TABLE 1
Spitzer & *IRAS* PHOTOMETRY OF HD 61005

Band	Wavelength[a] (μm)	Flux Density (mJy)	$\sigma_{\rm int}$ (mJy)	$\sigma_{\rm tot}$ [b] (mJy)	Instrument
3.6	3.535	755.06	...	16.21	*Spitzer*/IRAC
4.5	4.502	463.90	...	10.65	*Spitzer*/IRAC
8.0	7.735	172.45	...	3.68	*Spitzer*/IRAC
13[d]	13.17	62.34	...	3.08	*Spitzer*/IRS
24	23.68	41.49	...	1.70	*Spitzer*/MIPS
24[c,d]	24.02	45.53	...	2.80	*Spitzer*/IRS
33[c]	32.36	109.98	...	6.74	*Spitzer*/IRS
60[e]	60	446.5	28.3	28.3	*IRAS*
70	71.42	628.7	...	45.4	*Spitzer*/MIPS

[a]Weighted average wavelengths.

[b]The total uncertainty ($\sigma_{\rm tot}$) is the *rss* of the "internal" measurement uncertainty (precision) and the "calibration" uncertainties (accuracy).

[c]Synthetic band-pass photometry with 1.6, 4.7 and 5μm band-widths (FWHM) for 13, 24 and 33μm respectively.

[d]The MIPS 24μm photometry has not had a color-correction applied. The current value for the color-correction would yield $F_c = 1.014 \times F_{\rm obs} = 42.1$ mJy).

[e]A color correction $F_c = 0.717 \times F_{\rm obs}$ has been applied as per ***